AIAA JOURNAL
Vol. 43, No. 9, September 2005

Measurements of Flow Conductivity and Density Fluctuations in Supersonic Nonequilibrium Magnetohydrodynamic Flows

Rodney Meyer,* Munetake Nishihara,* Adam Hicks,* Naveen Chintala,* Michael Cundy,† Walter R. Lempert,‡ and Igor V. Adamovich§
The Ohio State University, Columbus, Ohio 43210
and
Sivaram Gogineni¶
Innovative Scientific Solutions, Inc., Dayton, Ohio 45440

A new blowdown nonequilibrium plasma magnetohydrodynamic (MHD) supersonic wind tunnel operated at complete steady state has been developed and tested at Ohio State. The wind tunnel can be operated at Mach numbers up to $M = 3$–4 and mass flow rates of up to 45 g/s at a stagnation pressure of 1 atm. Pitot tube and schlieren measurements in a $M = 3$ test section showed reasonably good flow quality, up to 80% inviscid core across the larger dimension and up to 50% inviscid core across the smaller dimension of the flow. Stable and diffuse transverse rf discharges (rf power up to 1 kW) have been sustained in $M = 3$ nitrogen flows, at magnetic fields of up to $B = 1.5$ T. Operation at higher magnetic fields produced a more uniform rf plasma in the MHD test section. Hall parameter and electric conductivity of the flow have been inferred from the dc (MHD) current and voltage measurements at different values of the magnetic field. At $B = 1.5$ T and rf power of 500 W, the Hall parameter is $\beta \cong 3$ and the conductivity is $\sigma \cong 0.05$ mho/m. At the rf power of 1 kW, the extrapolated conductivity is ∼0.1 mho/m. The results of the present work demonstrate the Lorentz force effect on the supersonic boundary layer in $M = 3$ flows of nitrogen ionized by a high-power transverse rf discharge in the presence of the magnetic field. Boundary-layer density fluctuation spectra are measured using the laser-differential-interferometry diagnostics. In particular, decelerating Lorentz force applied to the flow produces a well-reproduced increase of the density fluctuation intensity by up to 10–20% (1–2 dB), compared to the accelerating force of the same magnitude applied to the same flow. The effect is produced for two possible combinations of the magnetic field and MHD current directions producing the same Lorentz force direction (both for accelerating and decelerating force). The effect is observed to increase with the flow conductivity. On the other hand, the effect of Joule heating on the density fluctuation spectra appears insignificant.

I. Introduction

THE use of magnetohydrodynamics for supersonic flow control, supersonic airbreathing propulsion, and for development of novel hypersonic ground-testing facilities continues to attract considerable interest.[1–5] The most serious challenge in developing these applications is creating and sustaining electrical conductivity in the airflow sufficient to produce substantial MHD effects. The conductivity required to produce significant changes in the freestream flow enthalpy can be estimated from the magnetic interaction parameter:

$$I_{\mathrm{FS}} = \frac{\text{Lorentz force}}{\text{inertia force}} = \frac{\sigma B^2 L}{\rho U} \sim 1 \qquad (1)$$

where B is the magnetic field, L is the length of the MHD channel, ρ is the flow density, and U is the freestream flow velocity. Assuming $B \sim 10$ T, $L \sim 1$ m, $\rho \sim 0.01$–0.1 m^3 (for a room-temperature flow at $P \sim 0.01$–0.1 atm), and $U \sim 1000$ m/s, one obtains a conductivity of $\sigma \sim 0.1$–1.0 mho/m. Recent experimental and computational results suggest that such values of electrical conductivity in low-temperature supersonic flows can be achieved using efficient nonequilibrium ionization methods, such as high-energy electron beams or pulsed electric discharges.[6,7] The preceding estimate also suggests that noticeable MHD effects in cold supersonic flows can be produced only using powerful, large-scale superconducting magnets. Indeed, Eq. (1) suggests that for less powerful rare-Earth permanent magnets ($B \sim 1.0$–1.5 T) the required conductivity increases up to $\sigma \sim 10$–100 mho/m. However, such low-cost, relatively lightweight magnets can be usable for supersonic flow control applications that can be realized at lower values of electrical conductivity. Qualitatively, these applications might include control of turbulent transition in the supersonic ionized boundary layer and supersonic flow separation control, which both critically affect aerodynamic drag and heat transfer on a hypersonic vehicle. Indeed, in the boundary layer the appropriate characteristic velocity scale is the friction velocity, $u^+ = \sqrt{(\tau_w/\rho)} = U\sqrt{(c_f/2)} \approx 0.04U$. Here τ_w is the shear stress on the wall, and $c_f/2 = \tau_w/\rho U^2 \approx 0.03 \times Re_x^{-0.2}$ is the flat-plate turbulent boundary-layer skin-friction coefficient,[8] $c_f/2 = 1.9 \times 10^{-3}$ at $Re_x \sim 10^6$. Therefore, the boundary-layer magnetic interaction parameter can be expressed as

$$I_{\mathrm{BL}} = \frac{\text{Lorentz force}}{\text{inertia force}} = \frac{\sigma B^2 L}{\rho u^+} = \frac{\sigma B^2 L}{\rho U\sqrt{c_f/2}} \sim 1 \qquad (2)$$

which has been suggested in Refs. 9–11. Equation (2) suggests that the near-wall boundary-layer flow can be affected at significantly lower conductivity values, $\sigma \sim 0.3$–3.0 mho/m, which can be achieved in nonequilibrium plasma flows.

Presented as Paper 2004-0510 at the AIAA 42nd Aerospace Sciences Meeting, Reno, NV, 5–8 January 2004; received 29 September 2004; revision received 25 February 2005; accepted for publication 28 February 2005.

*Graduate Student, Nonequilibrium Thermodynamics Laboratories, Department of Mechanical Engineering.
†Undergraduate Student, Nonequilibrium Thermodynamics Laboratories, Department of Mechanical Engineering.
‡Professor, Nonequilibrium Thermodynamics Laboratories, Department of Mechanical Engineering. Associate Fellow AIAA.
§Associate Professor, Nonequilibrium Thermodynamics Laboratories, Department of Mechanical Engineering. Associate Fellow AIAA.
¶Vice President and Director of Marketing.

Boundary-layer transition control seems to be a particularly promising application of the MHD supersonic flow control concept because only relatively weak actuating forces might be needed to affect the flow instability development. Thus, the delay or acceleration of the transition can be achieved by suppression or enhancement of initial instability waves at an early stage of the boundary-layer flow development for the purpose of drag and heating reduction or for the purpose of fuel mixing enhancement. Because the disturbance waves are initially very weak, their control by magnetic forces might only require relatively weak electromagnetic fields and/or fairly low electrical conductivity in the gas flow. Similar qualitative arguments can be suggested with regard to flow separation control because the flow momentum in the vicinity of the separation and reattachment points is rather low, and affecting it might not require a significant Lorentz force. These arguments are consistent with results of experiments in a salt-water turbulent boundary layer,[9] which demonstrated possibility of both reduction and amplification of the turbulence intensity by Lorentz forces produced by permanent magnets, at a conductivity of $\sigma \sim 3$ mho/m. These results suggest the need for an experimental study of the feasibility of supersonic boundary-layer control using MHD body forces.

Previously, we have detected the MHD effect in a $M = 4$ helium nonequilibrium plasma flow with the magnetic field produced by a permanent magnet.[10] In Ref. 10, the fluctuation spectra have been measured by a microphone placed in the test-section wall. However, in the presence of high-power electric discharges and strong magnetic fields diagnostics involving microphones, pressure transducers, hot wires, etc. are subjected to significant electromagnetic interference. In many cases, electromagnetic shielding using a Faraday cage around the plasma section proves to be ineffective and for larger-scale tests appears to be impractical. Also, in Ref. 10 the flowfield in the test section (in particular, the boundary-layer thickness) was not well characterized. Recently, a new nonequilibrium plasma supersonic MHD wind-tunnel facility has been developed at Ohio State University. It is specifically designed for studies of MHD effects on turbulent transition in the boundary layer and on the supersonic flow separation, as well as control and stability of electric discharge plasmas in MHD test sections in the presence of transverse and axial electric fields and transverse magnetic field. Recent results obtained at this facility show that it produces stable, diffuse, and uniform plasma flows in the supersonic MHD test section, with good flow quality.[12–14] The main objective of the present work is detecting the Lorentz force effect on the supersonic ionized boundary-layer fluctuation spectra using optical diagnostics, which would greatly reduce electromagnetic interference from the plasma and the magnetic field.

II. Experimental

The experiments have been conducted at a new supersonic nonequilibrium plasma/MHD wind-tunnel facility at the Nonequilibrium Thermodynamics Laboratories. This facility generates stable, diffuse, good flow quality supersonic flows of nonequilibrium plasmas at $M = 3$–4 in a uniform magnetic field up to $B = 2$ T and can be operated continuously. Preliminary experimental results using this facility have been recently reported in Refs. 12–14. The schematic of the experiment is shown in Fig. 1. An aerodynamically contoured $M = 3$ supersonic nozzle made of transparent acrylic plastic is connected to a 2×4 cm rectangular cross-section test section 12 cm long and an angle step diffuser. The top and bottom walls of the test section are diverging at a 0.5-deg angle each to provide boundary-layer relief. The nozzle/test-section/diffuser assembly is attached to a vacuum system connected to a 1200-ft^3 dump tank pumped out by an Allis-Chalmers 1300 cfm rotary vane vacuum pump. The minimum pressure in the vacuum system sustained by the pump is 35–40 torr, which necessitates the use of a supersonic diffuser with the nozzle/test section operated at relatively low stagnation and static pressures ($P_0 = \frac{1}{3}$–1 atm, $P_{\text{test}} = 7$–20 torr). The nozzle assembly is equipped by three pressure taps measuring plenum pressure as well as static pressures at the beginning and at the end of the test section. The test section also has several pitot ports, shown in Fig. 1. The pitot tube probes can be moved in and out of the flow during the experiment, which allows pitot-pressure profile measurements in both horizontal and vertical planes. The nozzle-throat dimensions are 9.5×20 mm, which gives the mass flow rate through the test section of $\dot{m} = 15$ g/s at $P_0 = \frac{1}{3}$ atm and $\dot{m} = 45$ g/s at $P = 1$ atm.

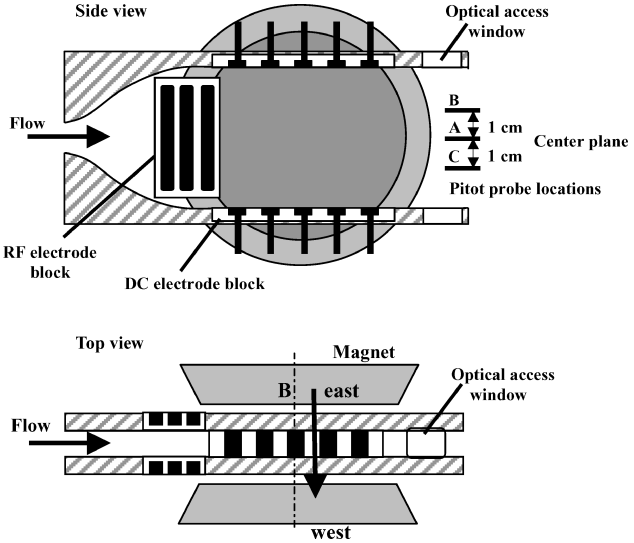

Fig. 1 Schematic of a $M = 3$ nozzle/test section.

Ionization in the $M = 3$ test section is produced by a transverse rf discharge sustained between two electrode blocks 3 cm long flush mounted in the side test-section walls (Fig. 1). Each electrode block, manufactured of high-temperature machinable mica ceramic, incorporates three copper strip electrodes 35 mm long and 5 mm wide. The electrodes are rounded at the edges to prevent high electric field concentration and "hot spot" formation in the plasma near the edges. The use of dielectric (ceramic) layers between the electrodes and the flow precludes secondary ionization from the electrode surfaces, which improves the stability of the transverse rf discharge sustained in the test section.[15] The rf discharge is produced using a 5-kW, 13.56-MHz Dressler power supply with an automatic impedance matching network. In the present experiments, very good impedance matching has been achieved for rf discharge powers up to 1 kW, with only about 1–3% of the input rf power reflected back. The entire nozzle/test-section/diffuser assembly was placed between the poles of a GMW water-cooled electromagnet, as shown in Fig. 1. The magnet can generate a steady-state magnetic field up to $B = 3.5$ T between two circular poles up to 25 cm in diameter. The magnetic field can be generated in two opposite directions transverse to the flow, shown as "east" and "west" in Fig. 1. In the present experiments, for the distance between the 15-cm-diam poles of 6–7 cm, the magnetic field at maximum current through the magnet coils of 140 A is up to $B = 1.7$–1.8 T. For relatively short run durations (of the order of tens of seconds), the magnetic field can be significantly increased by temporarily increasing the magnet current (up to $\sim$200 A) and chilling the cooling water.

The transverse dc electrical current (sustainer current) in the supersonic flow ionized by the rf discharge is sustained by applying a dc field (up to 500 V/cm) to two 50×20 mm dc electrode blocks flush mounted in the top and bottom nozzle walls 4 cm apart, perpendicular both to the flow velocity and to the magnetic field direction, as shown in Fig. 1. The applied dc field, which is far too low to produce additional ionization in the flow, except in the dc cathode layer, is needed to sustain transverse (MHD) current. Both continuous and sectioned electrode blocks have been made of high-temperature aluminum silicate ceramic with electrodes made of copper. The continuous copper electrodes are 45 mm long each. The sectioned electrode blocks consist of five copper electrode strips 5 mm long each. Sectioned electrodes would allow sustaining both transverse and axial dc electric fields in the test section. However, in the present work, only transverse dc field was applied to the sectioned electrodes, which were therefore short circuited within

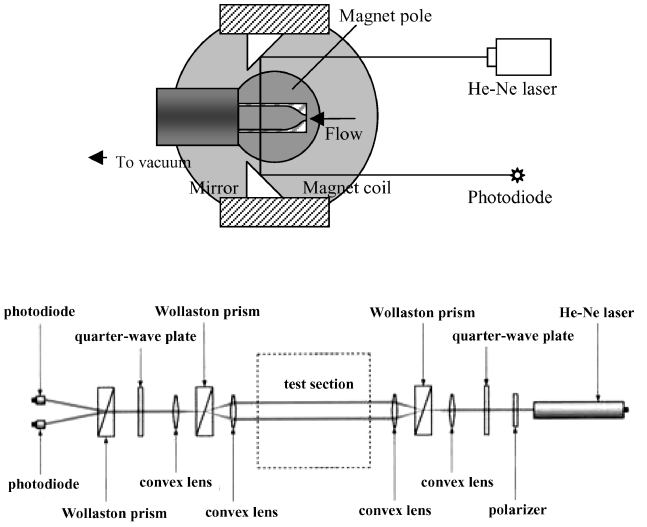

Fig. 2 Layout and schematic of the LDI diagnostics.

each dc electrode block. The dc field is applied using a DEL 2-kV/3-A power supply operated in a voltage stabilized mode, with a 0.5–5.0 kΩ ballast. RF ionization is produced approximately 2 cm upstream of the dc electrodes. Current in the dc sustainer circuit is measured using a Tektronix AM503S current probe.

Optical access to the flow is provided using two $1 \times 1/2$ in. (2.54×1.27 cm) glass windows in the top and bottom walls of the $M = 3$ test section (see Fig. 1). The windows are centered in the flow. Our previous pitot tube measurements showed that the side-wall boundary-layer thickness in $M = 3$, $P_0 = \frac{1}{3}$–1 atm flows is 5–8 mm (Ref. 12). Therefore, the test section provides optical access approximately to one-half of both side-wall boundary layers. Boundary layers in the $M = 3$ flow without plasmas are also visualized using a Z-type schlieren system with 1-kW continuous light source, 60-in.-focal-length spherical mirrors, and a high-resolution charge-coupled-device (CCD) camera.

MHD effect on a supersonic ionized boundary layer was studied using a laser-differential-interferometry (LDI) diagnostics described in greater detail in Ref. 16. Briefly, a plane polarized He–Ne laser beam (Coherent He-Ne laser, Model 31-2025) is split into two plane polarized beams using a quarter-wave plate and a Wollaston prism (Fig. 2) and sent through two different regions in the supersonic flow. The reference beam is passing through the flow along the centerline, and the probe beam is passing through the boundary layer. The resultant phase shift between the two beams is proportional to the line-of-sight averaged density difference along the beam paths. Therefore, Fourier transform of the resultant interference signal performed by the Stanford Research Systems (Model SR 785) Dynamic Signal Analyzer yields the boundary-layer density fluctuation spectrum (relative to the reference laser beam passing through the centerline of the flow). The location of the probe beam can be controlled by rotating the prism. LDI signal acquisition, averaging, and processing by the signal analyzer requires a steady-state flow run time of 1–5 s, depending on the number of averages. Typically, good signal to noise is achieved for the acquisition/processing times of 2–3 s.

One of the main objectives of the present work was to measure the effect of the Lorentz force on the low-temperature, ionized, supersonic boundary layer, in particular on the density fluctuation spectrum. Because in the present experiments the MHD loading parameter is quite high, $K = E_y/uB_z \sim 40$, the effect of Joule heat on the flow might be quite substantial, possibly exceeding the Lorentz force effect. For this reason, the LDI measurements are always performed at four sets of conditions, with the magnetic field turned on: 1) in a cold supersonic flow without plasmas; 2) in a rf-ionized flow without dc electric field applied, that is, when the time-averaged Lorentz force is zero; 3) in a rf-ionized flow with dc field applied, with the Lorentz force directed downstream; and 4) in a rf-ionized flow with dc field applied, with the Lorentz force directed upstream. The purpose of this approach was to isolate the possible MHD effect, which should depend on the Lorentz force direction, from the polarity-independent effect of Joule heat. Downstream and upstream Lorentz force was produced for both possible directions of the transverse B field by changing the polarity of the dc electric field. To evaluate run-to-run variation of the LDI spectra, several runs (2–4) have been conducted for each set of conditions.

III. Results and Discussion

A. Flowfield Characterization

Figure 3 shows the results of the pitot-pressure measurements in $M = 3$ airflows at three different stagnation pressures, $P_0 = 250$, 500, and 725 torr, at the downstream end of the test section (20 cm from the nozzle throat or 2 cm upstream of the diffuser). It can be seen that in all three cases the pitot-pressure distribution in the vertical plane is nearly uniform over about 80% of the flow (i.e., up to 16 mm distance from the centerline). In the horizontal plane, the pitot tube remains uniform over about 50% of the test section at $P_0 = 250$ torr and over about 35% of the test section at $P_0 = 500$ torr. In these two cases, the centerline pitot pressures correspond to Mach numbers of $M = 2.88$ and 2.84, respectively. This is consistent with Mach numbers inferred from the static-pressure measurements at the end of the test section, $P = 9.3$ torr, $M = 2.79$ at $P_0 = 250$ torr, and $P = 19.5$ torr, $M = 2.76$ at $P_0 = 500$ torr. The increase of the side-wall boundary-layer thickness with pressure is consistent with three-dimensional compressible Navier–Stokes turbulent flow calculations[17] and might possibly be an indication of boundary-layer transition over the range of Reynolds numbers tested.

Figure 4 shows additional pitot tube measurements in three horizontal planes at $P_0 = 250$ torr, A, at the centerline plane, B, 10 mm above the centerline plane, and C, 10 mm below the centerline plane. It can be seen that the pitot-pressure distribution across the centerline plane (location A) indicates a thicker boundary layer compared to the other two planes (B and C). In other words, these measurements suggest the presence of a bulge in the side-walls' boundary layers near the centerline plane, which might be caused by a secondary cross flow present in the rectangular cross-section test section.[18]

Figure 5 shows a schlieren image of the flow in the test section (20 cm from the nozzle throat or 2 cm upstream of the diffuser, looking top to bottom), at stagnation pressure of $P_0 = 250$ torr. The light areas on both sides of the flow are boundary-layer regions. It can be seen that the size of the core flow is approximately 30% of the distance between the side walls of the test section, which is consistent with the pitot probe measurements (see Fig. 4).

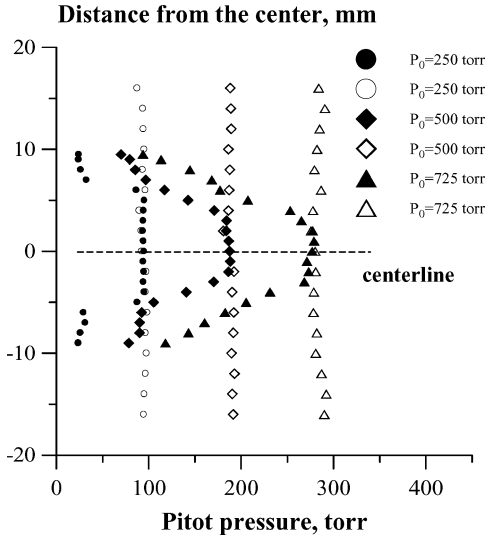

Fig. 3 Summary of pitot-pressure measurements in horizontal and vertical centerline planes at different stagnation pressures: air, $M = 3$; ●, ◆, ▲, horizontal plane; ○, ◇, △, vertical plane.

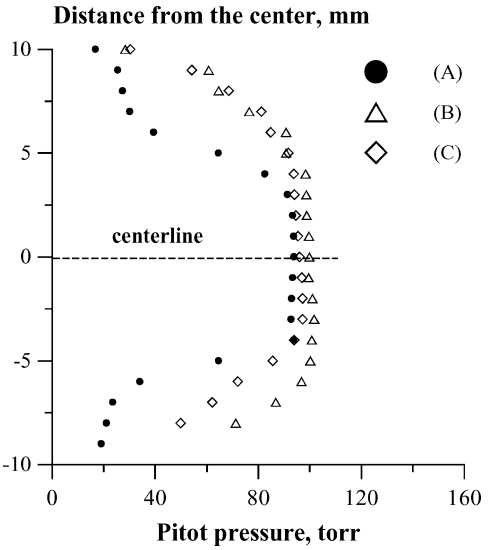

Fig. 4 Pitot-pressure measurements in the horizontal centerline plane (A), 10 mm above the centerline plane (B), and 10 mm below the centerline plane (C), at stagnation pressure of $P_0 = 250$ torr: air, $M = 3$.

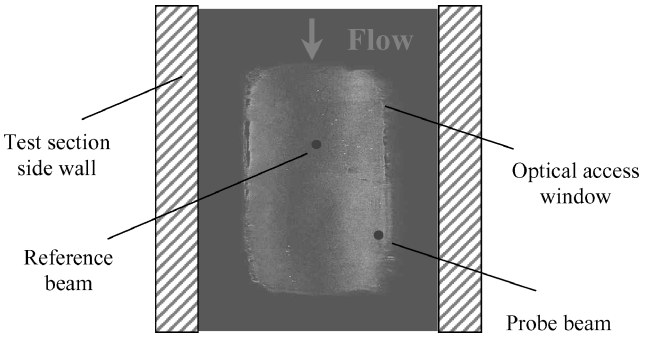

Fig. 5 Schlieren image of the $M = 3$ flow in nitrogen ($P_0 = 250$ torr, no plasmas), with the schematic of the LDI laser beam arrangement in the flow. Lighter boundary-layer regions on both sides are clearly visible.

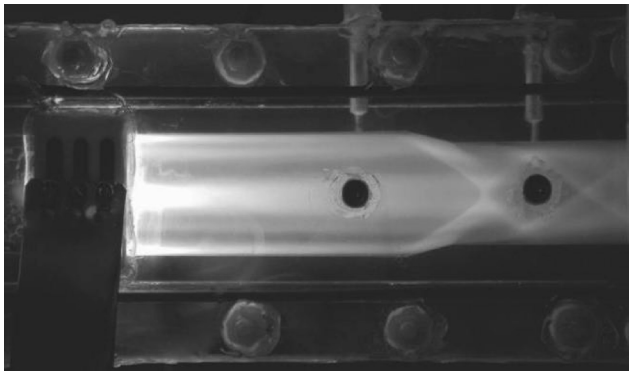

Fig. 6 500-W rf discharge in a $M = 3$ flows of nitrogen ($P_0 = 318$ torr, $P_{test} = 11.6$ torr, $I_{RMS} = 1.6$ A, $U_{RMS} = 3.7$ kV). The flow is left to right. Oblique shock train in the diffuser is clearly visible.

B. Electrical Measurements

Figure 6 shows a photograph of transverse 500-W rf discharge in the $M = 3$ flow of nitrogen at the plenum pressure of $P_0 = 318$ torr ($P_{test} = 11.6$ torr), with the test section mounted to the vacuum flange outside the magnet. At these conditions, the rms rf voltage and current are $I_{RMS} = 1.6$ A and $U_{RMS} = 3.7$ kV, respectively. It can be seen that the diffuse discharge occupies nearly the entire region between the rf blocks. The rf plasma glow is more intense in the center of the flow (because of a stronger electric field near the center of the electrode assembly) and near the top and bottom test-section walls (because of a longer flow residence time and lower density in the boundary layers, which can result in preferential ionization there). The rf afterglow plasma is quite long (at least 20 cm) and is extending into the diffuser, where it visualizes the oblique shock pattern (Fig. 6). The plasma flow visualization of shock waves, boundary layers, and wakes, also observed in our previous experiments,[19–21] can be used to study the possible MHD effect on the supersonic flow separation.

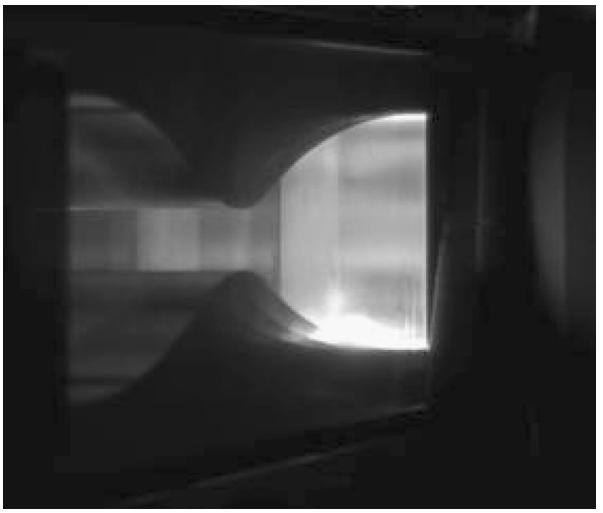

Fig. 7 Photograph of a crossed discharge (rf + dc) in a $M = 3$ nitrogen flow in magnetic field: nitrogen, $P_0 = 270$ torr, rf power 500-W, dc voltage $U_{PS} = 1500$ V, $B = 1.5$ T, $I_{DC} = 128$ mA. Flow is left to right.

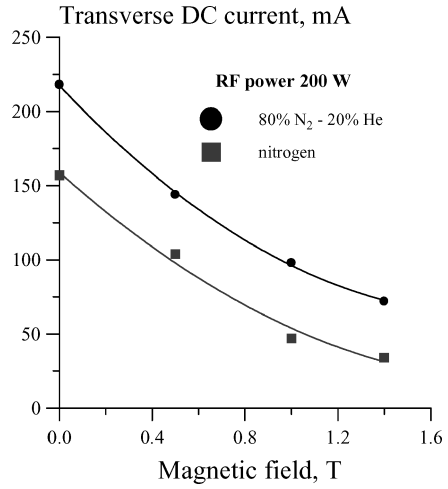

Fig. 8 Transverse dc current in $M = 3$ flows of a N_2–He mixture and nitrogen as functions of the magnetic field: $P_0 = 270$ torr, rf power 200 W, dc power supply voltage $U_{PS} = 1400$ V.

Figure 7 shows a photograph of crossed transverse discharges (rf + dc) sustained in a supersonic flow of nitrogen ($M = 3$, $P_0 = 270$ torr), in the presence of transverse magnetic field of $B = 1.5$ T. The flow is photographed at a sharp oblique angle from the nozzle plenum side. The rf discharge power is 500 W, and the dc power supply voltage is $U_{PS} = 1500$ V (with a 5.2-kΩ ballast resistor in series with the discharge electrodes). It can be seen that the plasma in the MHD test section is diffuse, filling essentially the entire volume between the electrodes. A bright region near the bottom of the flow might be caused by preferential ionization in the bottom-wall boundary layer, as also suggested by Fig. 6. At these conditions, the measured dc sustainer current is $I_y = 128$ mA. It was also found that increasing the magnetic field in the range $B = 0$ to 1.5 T considerably improves the plasma stability and makes it more uniform and diffuse.

Figure 8 shows results of transverse dc current measurements in $M = 3$ flows of an 80% $N_2 - 20\%$ He mixture and pure nitrogen

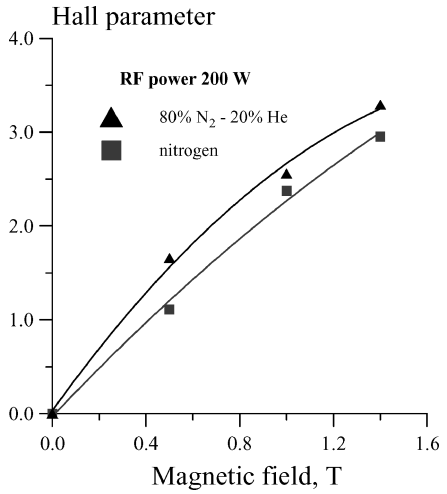

Fig. 9 Hall parameters in $M = 3$ flows of a N_2–He mixture and nitrogen as functions of the magnetic field for the conditions of Fig. 9.

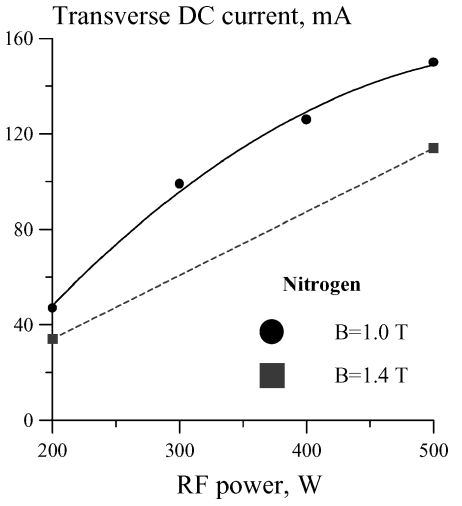

Fig. 10 Transverse dc current in $M = 3$ flows of nitrogen as functions of the rf discharge power: $P_0 = 270$ torr, dc power supply voltage $U_{PS} = 1400$ V.

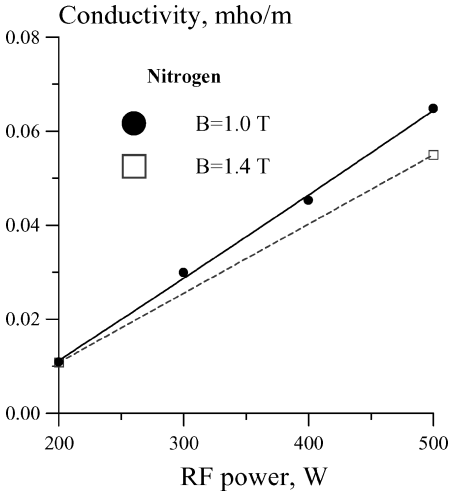

Fig. 11 Electric conductivity of $M = 3$ flows of nitrogen as a function of the rf discharge power for the conditions of Fig. 11.

as functions of the applied magnetic field. In these measurements, plenum pressure was $P_0 = 270$ torr (test-section static pressure $P = 12$ torr), rf power was 200 W, dc power supply voltage $U_{PS} = 1400$ V, and the ballast resistance was $R = 5.2$ kΩ. It can be seen that with all other conditions being the same, the current decreases with the magnetic field. This is the result of the Hall effect, which in the absence of the axial electric field reduces the transverse current component I_y and generates the axial current I_x (Ref. 22):

$$I_y = [\sigma/(1+\beta^2)](E_y - uB_z)A$$

$$I_x = \beta[\sigma/(1+\beta^2)](E_y - uB_z)A \qquad (3)$$

In Eqs. (3), σ is the scalar electric conductivity, $A = 10$ cm^2 is the total surface area of the dc electrodes, and $\beta = eB_z/m_e\nu_{en}$ is the Hall parameter, that is, the ratio of the electron cyclotron frequency eB_z/m_e to the electron-neutral collision frequency ν_{en}. Note that the factor uB_z in Eqs. (3) can be neglected compared to the transverse electric field E_y because of high values of the MHD loading parameter, $K = E_y/uB_z \sim 40$, under the present conditions. Transverse electric field in Eqs. (3) is estimated as $E_y \cong (U_{PS} - I_y R)/h$, where $h = 4$ cm is the test-section height. Assuming that the scalar electric conductivity σ is independent of the magnetic field, the results shown in Fig. 8 can be used to infer the values of the apparent Hall parameter at these conditions, using the first of Eqs. (3). The results, plotted in Fig. 9, show that the Hall parameter reaches $\beta \approx 3$ at $B = 1.4$ T. This is consistent with the theoretical value of the Hall parameter for the electron collision frequency in nitrogen at $N = 8 \times 10^{17}$ cm^{-3} and $E_y/N = (2\text{–}4) \times 10^{-16}$ V · cm^2, calculated from the solution of Boltzmann equation for plasma electrons at these conditions, $\nu_{coll} = (5.3\text{–}6.1) \times 10^{10}$ s^{-1}, $\beta = 4.0\text{–}4.6$ at $B = 1.4$ T (Ref. 3). More accurate Hall parameter measurements can be obtained by measuring the axial and the transverse voltages E_x and E_y, using sectioned MHD electrodes.

Figure 10 shows the results of the transverse dc current measurements in $M = 3$ nitrogen flows as a function of the rf discharge power, at two values of magnetic field, $B = 1.0$ and 1.4 T. In these measurements, again both the dc power supply voltage and the ballast resistance were kept the same, $U_{PS} = 1400$ V and $R = 5.2$ kΩ. It can be seen that the current increases with the rf power, up to $I_y = 100\text{–}150$ mA at 500 W, which is caused by the increased conductivity of the plasma in the rf discharge. Because the dependence of the apparent Hall parameters on the magnetic field (at the same conductivity) has already been determined from the results of Fig. 9, the data of Fig. 10 can now be used to infer the electric conductivity of the flow in the MHD test section at these conditions (at the same magnetic field), using the first Eq. (3). The results are summarized in Fig. 11. One can see that the conductivity considerably increases with the rf power, up to $\sigma = 0.05$ mho/m. Extrapolating these results to the rf power of ~1 kW, easily attainable at the present MHD facility, gives $\sigma \sim 0.1$ mho/m. Note that the present procedure for calculating the conductivity neglects the dc cathode voltage drop, which results in a somewhat underestimated conductivity value. Assuming normal current density in the cathode layer, the cathode voltage drop in a nitrogen glow discharge with a copper cathode is $U_{cathode} \sim 200$ V (Ref. 15). At the present conditions, such cathode fall would underestimate the nitrogen flow conductivity up to 15–30%.

As shown in our recent experiments,[23] further conductivity increase, without significantly raising the ionization source power, can be achieved by replacing the sine-wave rf plasma generator with a repetitively pulsed (up to 50 kHz), short pulse duration (10–20 ns), high-voltage (20–30 kV) power supply. Nonequilibrium plasma generated by such pulsed power sources has a much larger fraction of the input power going to ionization,[15] which considerably increases the plasma conductivity at a comparable discharge power budget. The short pulse duration and a very low duty cycle, ~1/1000, also preclude plasma instability development, which greatly improves stability of these plasmas at high currents. Therefore, the use of the repetitively pulsed ionization is expected to produce a more pronounced Lorentz force effect on the flow.

It appears that electrical conductivity of $\sigma = 0.05$ mho/m should make possible sustaining rather high dc currents in the MHD test section, on condition that the Hall effect is mitigated (i.e., in the Faraday

configuration). Indeed, from the data of Figs. 10 and 11, at $B = 1.4$ T and $U_y = U_{PS} - I_y R \sim 800$ V (transverse field of $E_y \sim 200$ V/cm), the transverse current should be $I_y \sim 1$ A. However, the actual conductivity and current values for this electrode configuration are lower by a factor $(1 + \beta^2) \cong 10$, that is, by an order of magnitude (see Fig. 10). Transverse current reduction caused by the Hall effect can be mitigated by applying an axial electric field E_x in order to cancel the axial current J_x [see Eqs. (3)]. This can be achieved by individually ballasting the sectioned MHD electrodes (see Fig. 1). However, because of the small MHD channel length-to-height ratio of only 5 cm/4 cm = 1.25, the axial electric field in this case can be limited to the near-electrode areas and can be rather weak far from the MHD electrodes, that is, in the core flow.

C. LDI Measurements

Figure 12 shows the LDI spectra taken in a $M = 3$ nitrogen flow at the baseline plenum pressure of $P_0 = 250$ torr, that is, at the conditions of Fig. 5. The probe laser beam is located midway between the wall and the centerline, as shown in Fig. 5. The two groups of spectra shown in Fig. 12 are both measured in the presence of $B = 1.5$ magnetic field 1) in the flow without plasmas and 2) in the rf-ionized flow without the dc field applied. In both these cases, there is no net Lorentz force applied to the flow, whereas in case 2 there is Joule heating of the flow by the 500-W rf discharge. Typically, the raw LDI spectra have a run-to-run intensity variation of up to 1–2 dB, which is most likely caused by the effect of magnetic field on the mirror holder assembly mounting the mirrors to the magnet frame, which affects the LDI beam alignment. Therefore, in the present paper the raw LDI spectra have been normalized (i.e., shifted up or down on a log-log scale) to match their intensities at the same conditions. Note that such intensity normalization did not affect the shape of the spectra. From Fig. 12, which shows two spectra for each set of conditions, it can be seen that the shape of the intensity-matched spectra has a very good run-to-run reproducibility, typically within 0.5–1.0 dB. Also, the results of Fig. 12 show that the cold-flow spectra and the rf-ionized flow spectra (without the dc field applied) are very nearly identical. This suggests that the effect of Joule heating on the boundary-layer density fluctuations at these conditions is small.

Note that the shape of the LDI spectra, that is, a nearly flat-plateau followed by a roll-off is qualitatively consistent with the in-flight supersonic boundary-layer measurement,[24] shown in Fig. 13. In the present measurements, the roll-off begins at the dimensionless frequency of $\omega^* = \omega\delta/U_0 \sim 2\pi \times 40$ kHz $\times$ 0.5 cm/600 m/s ~ 2, which is again consistent with the results of Ref. 24.

Figure 14 shows the LDI spectra at the same flow conditions, for sets 3 and 4, that is, in a rf-ionized flow with dc field applied, for the accelerating Lorentz force, and in a rf-ionized flow with dc

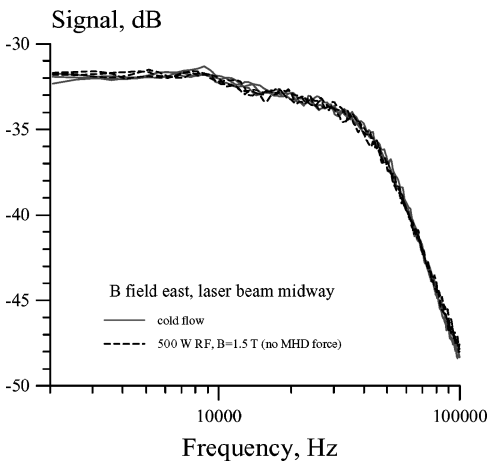

Fig. 12 Overlapped LDI spectra in $M = 3$ flows of nitrogen ($P_0 = 250$ torr, $B = 1.5$ T, rf power 500 W), for the cold flow without plasmas and for the rf-ionized flow. No dc field and Lorentz force applied.

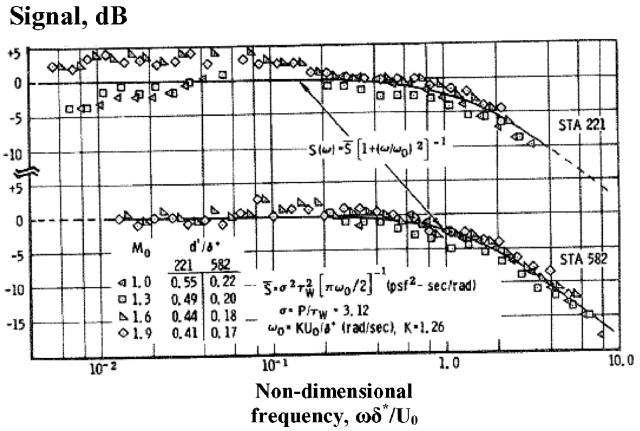

Fig. 13 Pressure fluctuation spectra in a supersonic boundary layer at $M = 1.0$–1.9. Flight measurements at 221 in. (top curve) and 582 in. (bottom curve) aft from the nose of a flight vehicle.[24]

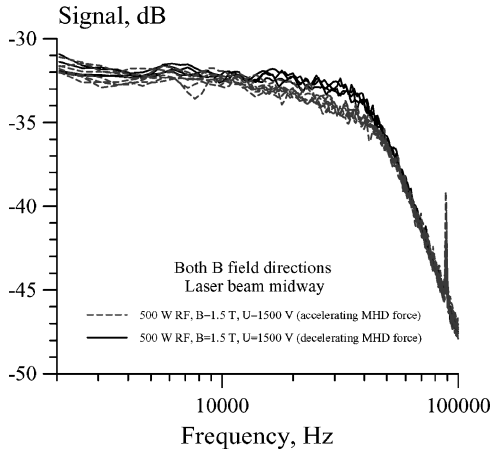

Fig. 14 Overlapped LDI spectra in $M = 3$ flows of nitrogen ($P_0 = 250$ torr, $B = 1.5$ T, rf power 500 W, $U_{DC} = 1500$ V) for the downstream Lorentz force (six runs) and the upstream Lorentz force (four runs). In both cases, the Lorentz force is produced for two opposite directions of the B field by flipping the dc electric field.

field applied, for the decelerating Lorentz force. (Several runs are shown for each set.) Note that in this series of experiments, both accelerating and decelerating Lorentz force within each set have been produced for two opposite directions of the magnetic field ($B = 1.5$ T) by changing the dc voltage polarity ($U_{PS} = 1500$ V, ballast resistor 1 kΩ). Again, one can see that reproducibility of the shape of the spectra for each set is very good, below 1 dB. It can also be seen that Fig. 14 shows small (~2 dB) but consistently reproduced difference between the spectra for the accelerating (set 3) and decelerating (set 4) Lorentz force. In particular, the fluctuation intensity in the entire plateau from 2 to 40 kHz is higher in the flow with the decelerating Lorentz force. This is consistent with the results obtained in the salt-water boundary layer,[9] where decelerating Lorentz force was shown to amplify turbulent fluctuations while accelerating force reduced them. Also, in the present experiments the fluctuation intensity increase has been observed for both possible B and E field configurations giving the same upstream Lorentz force direction, which suggests this to be a true MHD effect.

Figure 15 shows the LDI spectra for the accelerating and decelerating Lorentz force, at the same conditions as in Fig. 14, but at higher rf discharge powers, 0.75 and 1 kW. For both series of experiments, the results of two runs are shown for every set of conditions, to demonstrate good run-to-run reproducibility. In this case, again, the effect of density fluctuation increase in the presence of decelerating Lorentz force has been detected for both magnetic field directions (east and west, as shown in Fig. 1). It can be seen that in the region

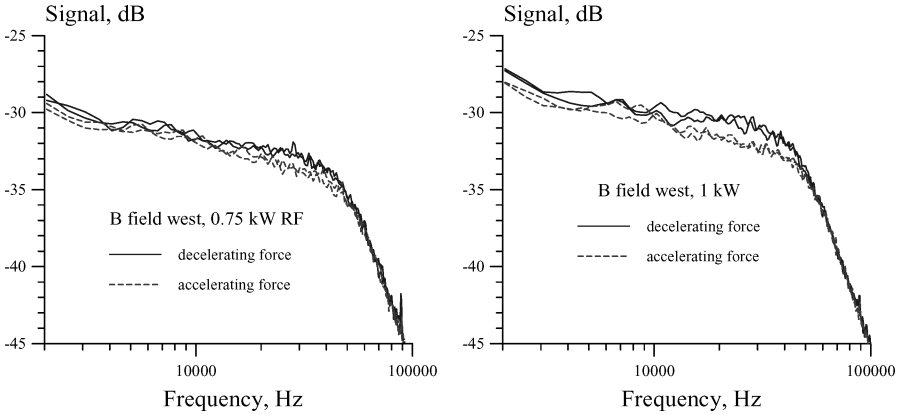

Fig. 15 LDI spectra in $M = 3$ flows of nitrogen ($P_0 = 250$ torr, $B = 1.5$ T) for accelerating and decelerating Lorentz force directions at rf powers of 0.75 and 1.0 kW. For all sets of conditions, the results of two runs are shown.

from about 15 to 50 kHz the fluctuation intensity for the decelerating Lorentz force is higher by about 1 dB at rf power of 0.75 kW and by about 2 dB at the rf power of 1 kW (Fig. 15). Note that when the rf power increases from 0.75 to 1 kW (i.e., by 33%), the transverse dc current increases by about 10–15%, from 180–200 mA to 200–230 mA, depending on the B field and dc electric field polarity.

To summarize, the results of Figs. 12, 14, and 15 consistently show the well-reproduced amplifying effect of decelerating Lorentz force on the boundary-layer density fluctuations, which increases with the flow conductivity and is not related to Joule heating. However, additional experiments are needed to determine whether MHD forcing directly affects density fluctuations in the ionized flow, or the effect is indirect, such as Lorentz force modification of the secondary cross flow in the side-wall boundary layer.

IV. Summary

The new blowdown nonequilibrium plasma MHD supersonic wind tunnel operated at complete steady state has been developed and tested. The wind tunnel can be operated at Mach numbers up to $M = 3$–4, at mass flow rates of up to $\dot{m} = 45$ g/s at $P_0 = 1$ atm. Pitot tube and schlieren measurements in a $M = 3$ test section showed reasonably good flow quality, up to 80% inviscid core across the larger dimension and up to 50% inviscid core across the smaller dimension of the flow. Stable and diffuse transverse rf discharges (rf power up to 1 kW) have been sustained in $M = 3$ nitrogen flows, at magnetic fields of up to $B = 1.5$ T. Operation at higher magnetic fields results in a more uniform rf plasma in the MHD test section. Hall parameter and electric conductivity of the flow have been inferred from the dc (MHD) current and voltage measurements at different values of the magnetic field. At $B = 1.5$ T and rf power of 500 W, the Hall parameter is $\beta \cong 3$, and the conductivity is $\sigma \cong 0.05$ mho/m. At the rf power of 1 kW, the extrapolated conductivity is ~ 0.1 mho/m.

The results of the present work demonstrate the Lorentz force effect on the supersonic boundary layer in $M = 3$ flows of nitrogen ionized by a high-power transverse rf discharge in the presence of the magnetic field. Boundary-layer density fluctuation spectra are measured using the laser-differential-interferometry diagnostics. In particular, decelerating Lorentz force applied to the flow produces a well-reproduced increase of the density fluctuation intensity by up to 10–20% (1–2 dB), compared to the accelerating force of the same magnitude applied to the same flow. The effect is produced for two possible combinations of the magnetic field and current directions producing the same Lorentz force direction (both for accelerating and decelerating force). The effect is observed to increase with the flow conductivity. On the other hand, the effect of Joule heating on the fluctuation spectra appears insignificant.

Further experiments to characterize the flowfield in the test section, in particular, to determine the state of the boundary layer are currently underway.

Acknowledgments

This research has been supported Air Force Office of Scientific Research Grant F49620-02-1-0164 and Phase II Small Business Innovative Research Grant F33615-01-C-3112 of the Air Vehicles Directorate of the Air Force Research Laboratory. We express our sincere gratitude to Bill Rich, Yurii Utkin, and Bryan Bystricky for numerous fruitful discussions and help with the experiment.

References

[1]Fraishtadt, V. L., Kuranov, A. L., and Sheikin, E. G., "Use of MHD Systems in Hypersonic Aircraft," *Technical Physics*, Vol. 43, No. 11, 1998, pp. 1309–1314.

[2]Kuranov, A. L., and Sheikin, E. G., "Magnetohydrodynamic Control on Hypersonic Aircraft Under Ajax Concept," *Journal of Spacecraft and Rockets*, Vol. 40, No. 2, 2003, pp. 174–182.

[3]Adamovich, I. V., Rich, J. W., and Nelson, G. L., "Feasibility Study of Magnetohydrodynamics Acceleration of Unseeded and Seeded Air Flows," *AIAA Journal*, Vol. 36, No. 4, 1998, pp. 590–597.

[4]Macheret, S. O., Shneider, M. N., and Miles, R. B., "Magnetohydrodynamic Control of Hypersonic Flow and Scramjet Inlets Using Electron Beam Ionization," *AIAA Journal*, Vol. 40, No. 1, 2002, pp. 74–81.

[5]Park, C., Mehta, U. B., and Bogdanoff, D. W., "Magnetohydrodynamic Energy Bypass Scramjet Performance with Real Gas Effects," *Journal of Propulsion and Power*, Vol. 17, No. 5, 2001, pp. 1049–1057.

[6]Macheret, S. O., Shneider, M. N., Miles, R. B., and Lipinski, R. J., "Electron-Beam-Generated Plasmas in Hypersonic Magnetohydrodynamic Channels," *AIAA Journal*, Vol. 39, No. 6, 2001, pp. 1127–1136.

[7]Macheret, S. O., Shneider, M. N., and Miles, R. B., "MHD Power Extraction from Cold Hypersonic Air Flow with External Ionizers," *Journal of Propulsion and Power*, Vol. 18, No. 2, 2002, pp. 424–431.

[8]Schlichting, H., *Boundary Layer Theory*, McGraw–Hill, New York, 1968, Chap. 21.

[9]Henoch, C., and Stace, J., "Experimental Investigation of a Salt Water Turbulent Boundary Layer Modified by an Applied Streamwise Magnetohydrodynamic Body Force," *Physics of Fluids*, Vol. 7, No. 6, 1995, pp. 1371–1383.

[10]Palm, P., Meyer, R., Ploenjes, E., Bezant, A., Adamovich, I. V., Rich, J. W., and Gogineni, S., "MHD Effect on a Supersonic Weakly Ionized Flow," AIAA Paper 2002-2246, May 2002.

[11]Macheret, S. O., Shneider, M. N., and Miles, R. B., "Magnetohydrodynamic and Electrohydrodynamic Control of Hypersonic Flows of Weakly Ionized Plasmas," *AIAA Journal*, Vol. 42, No. 7, 2004, pp. 1378–1387.

[12]Meyer, R., McEldowney, B., Chintala, N., Palm, P., and Adamovich, I. V., "Experimental Studies of Plasma Assisted Ignition and MHD Supersonic Flow Control," AIAA Paper 2003-0873, Jan. 2003.

[13]McEldowney, B., Meyer, R., Chintala, N., and Adamovich, I. V., "Measurements of Electrical Parameters of a Supersonic Nonequilibrium MHD Channel," AIAA Paper 2003-4279, June 2003.

[14]Meyer, R., Chintala, N., Bystricky, B., Hicks, A., Cundy, M., Lempert, W. R., and Adamovich, I. V., "Lorentz Force Effect on a Supersonic Ionized Boundary Layer," AIAA Paper 2004-0510, Jan. 2004.

[15]Raizer, Y. P., *Gas Discharge Physics*, Springer-Verlag, Berlin, 1991, Chap. 13.

[16]Salyer, T. R., Collicott, S. H., and Schneider, S. P., "Feedback Stabilized Laser Differential Interferometry for Supersonic Blunt Body Receptivity Experiments," AIAA Paper 2000-0846, Jan. 2000.

[17]McMullan, R. J., Lindsey, M. F., Adamovich, I. V., and Nishihara, M., "Experimental Validation of a 3-D Magnetogasdynamic Compressible Navier–Stokes Solver," AIAA Paper 2004-2269, June–July 2004.

[18]Rawat, P., Zhong, X., Singh, V., and Gogineni, S., "Numerical Simulation of Secondary Flow in a Weakly Ionized Supersonic Flow with Applied Electromagnetic Field," AIAA Paper 2005-5050, June 2005.

[19]Yano, R., Contini, V., Ploenjes, E., Palm, P., Merriman, S., Aithal, S., Adamovich, I., Lempert, W., Subramaniam, V., and Rich, J. W., "Supersonic Nonequilibrium Plasma Wind Tunnel Measurements of Shock Modification and Flow Visualization," *AIAA Journal*, Vol. 38, No. 10, 2000, pp. 1879–1888.

[20]Merriman, S., Ploenjes, E., Palm, P., and Adamovich, I. V., "Shock Wave Control by Nonequilibrium Plasmas in Cold Supersonic Gas Flows," *AIAA Journal*, Vol. 39, No. 8, 2001, pp. 1547–1552.

[21]Meyer, R., Palm, P., Plonjes, E., Rich, J. W., and Adamovich, I. V., "The Effect of a Nonequilibrium RF Discharge Plasma on a Conical Shock Wave in a $M = 2.5$ Flow," *AIAA Journal*, Vol. 41, No. 5, 2003, pp. 465–469.

[22]Rosa, R. J., *Magnetohydrodynamic Energy Conversion*, McGraw–Hill, New York, 1968, Chap. 1.

[23]Nishihara, M., Meyer, R., Cundy, M., Lempert, W. R., and Adamovich, I. V., "Development and Operation of a Supersonic Nonequilibrium MHD Channel," AIAA Paper 2004-2441, June–July 2004.

[24]Belcher, P. M., "Predictions of Boundary Layer Turbulence Spectra and Correlations for Supersonic Flight," 8 Congres International d'Acoustique, Sept. 1965.

M. Auweter-Kurtz
Associate Editor